Mechanism of $^{20}Ne(t,p)$ and nuclear structure of ^{22}Ne

Z. Q. Mao and H. T. Fortune
Department of Physics, University of Pennsylvania, Philadelphia, Pennsylvania 19104
(Received 18 February 1994)

In the $^{20}Ne(t,p)^{22}Ne$ reaction at a bombarding energy of 15 MeV, excitation energies have been measured for 81 levels up to $E_x = 13.4$ MeV. Thirteen new levels were identified. Distorted-wave Born-approximation (DWBA) calculations with spherical and deformed potentials were used to analyze the angular distributions. Two-step processes were found to make important contributions to the reaction. For most low-lying positive-parity levels, results are analyzed with two-particle transfer amplitudes from a realistic shell-model calculation. We have assigned spin-parities to 42 levels above 6.6 MeV based on the success of the DWBA analysis.

PACS number(s): 21.10.Hw, 21.60.Cs, 25.55.Hp, 27.30.+t

I. INTRODUCTION

Early analyses of (t,p) reactions using the microscopic distorted-wave Born-approximation (DWBA) assumed: (1) spherical optical potentials; and (2) final levels being populated through a direct one-step reaction mechanism. The DWBA under the above assumptions has successfully predicted the differential cross sections of the strongly populated levels for many direct reactions, e.g., in Refs. [1–4]. However, it often failed to explain the angular distributions of weakly populated final levels [5,6]. This failure was more obvious when reactions involved deformed targets and residual nuclei, such as in the $^{20}Ne(t,p)^{22}Ne$ reaction [6].

For deformed nuclei, inelastic-scattering cross sections are comparable with elastic scattering ones. Therefore, (t,p) reactions might be affected by inelastic scattering through channel coupling. The large inelastic-scattering cross sections could also enhance cross sections from two-step processes in (t,p) reactions. Thus, two-step processes might play an important role in reactions for which the one-step process is suppressed because of small one-step spectroscopic amplitudes or violation of selection rules.

If the transfer amplitudes of different components to a final level are known, one can obtain information about the reaction mechanism by comparing the theoretical cross section to the experimental one. The shell model has been widely used to calculate many properties, including transfer amplitudes of direct reactions, of 1p and 2s1d shell nuclei. For example, shell-model calculations using the USD interaction of Wildenthal [7] have been remarkably successful for predicting many features of 2s1d nuclei.

In the present work, we chose $^{20}Ne(t,p)^{22}Ne$ to study the (t,p) reaction mechanism, because both ^{20}Ne and ^{22}Ne are deformed nuclei and in the 2s1d shell. At an incident energy of 15 MeV, a previous study of this reaction showed strong direct reaction character [6]. However, in that work, angular distributions of many levels were poorly fitted.

II. EXPERIMENTAL PROCEDURE AND RESULTS

A 15-MeV triton beam was accelerated using the FN tandem Van de Graaff accelerator at the University of Pennsylvania. Outgoing protons were momentum analyzed with a multiangle spectrograph, and recorded on Ilford K-5 nuclear emulsion plates in the laboratory angular range of 7.5° to 82.5°, with 7.5° steps. Heavier particles were absorbed by Mylar absorbers directly in front of the nuclear emulsion plates. The ^{20}Ne target was gas in a closed rotating cell containing isotopically enriched ^{20}Ne (99.99%). The gas cell had a 250 $\mu g/cm^2$ aluminum window. Cell pressure was maintained at 45 ± 1 Torr. Indirect monitoring of the cell pressure was achieved by measuring elastically-scattered tritons in a Si surface barrier detector mounted at a laboratory angle of 30°.

Figure 1 displays a proton spectrum at $\theta_{lab} = 7.5°$. Experimental energy resolution was about 20 keV full width at half maximum (FWHM). Excitation energies were obtained from the average peak positions at all angles. Standard deviations of the excitation energies were about 5 keV for low-lying levels and 10–20 keV for higher-lying levels. We obtained excitation energies for 81 levels, including 13 that were previously unidentified, in ^{22}Ne. A few impurity peaks observed were due to the (t,p) reactions on ^{1}H, ^{12}C, and ^{16}O. The broad bumps near plate positions 550 mm and 400 mm are not real peaks, but arise from the structure of the gas-cell supports. Peaks in Fig. 1 are labeled with their excitation energies. Tables I and II list our measured excitation energies and their standard deviations, compared with those from previous measurements [6,8,9].

Absolute cross sections were calculated using known cell geometry, gas pressure, and integrated beam current. Relative uncertainties were taken to be the larger of 5% or the statistical uncertainty. The absolute scale is probably accurate to ±10%. Figures 2–8 contain the angular distributions of the (t,p) differential cross sections for all the 81 identified levels.

 ©1994 The American Physical Society

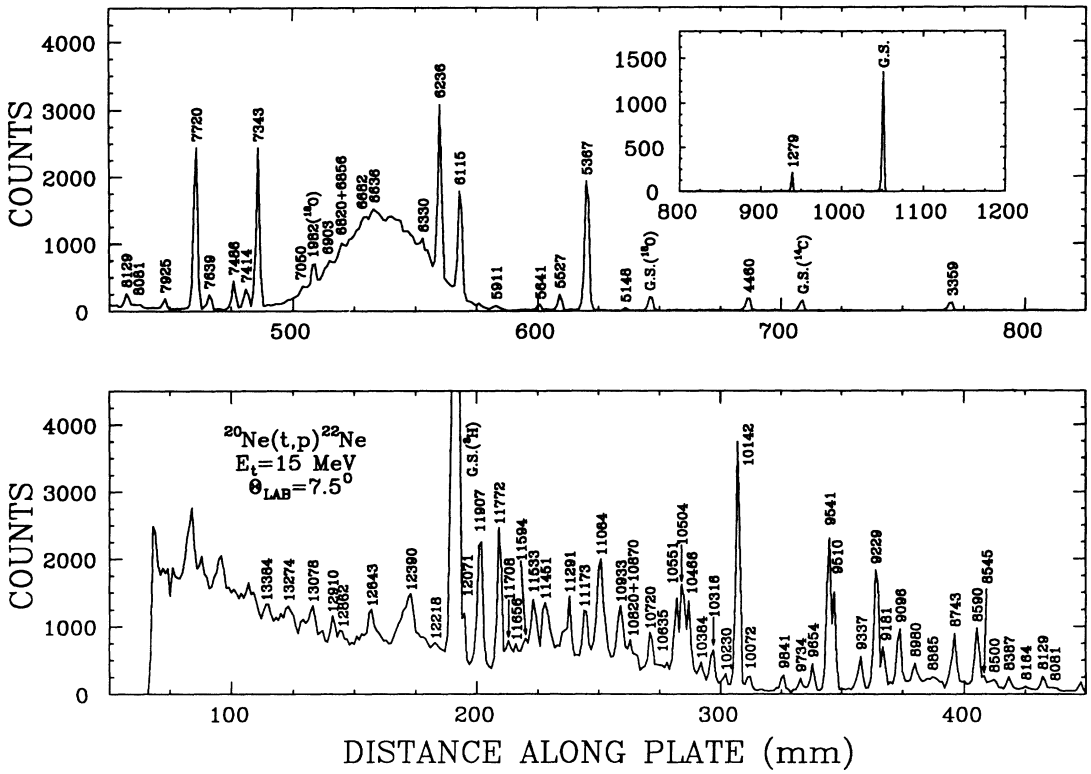

FIG. 1. Spectrum of the ^{20}Ne(t,p) reaction at a bombarding energy of 15 MeV and a laboratory angle of 7.5°. Peaks are labeled with their excitation energies. Excitation energies and their standard deviations are listed in Tables I and II.

III. ANALYSIS

Theoretical calculations of the ^{20}Ne(t,p) reaction were performed using codes DWUCK [10] and CHUCK [11]. These two codes calculate direct-reaction cross sections using the DWBA and residual interaction form of

$$V_0\delta\left(\vec{p}-\frac{\vec{n}_1+\vec{n}_2}{2}\right), \quad (1)$$

where V_0 is the interaction strength, and $\vec{p}$, $\vec{n}_1$, and $\vec{n}_2$ are the coordinates of transfered proton and neutrons, respectively. The triton optical potential parameters, obtained from elastic-scattering measurements of tritons at 15 MeV on ^{24}Mg [12], were used in conjunction with proton parameters [13] of Perey geometry [14] in the present work. This set of parameters was successfully used to analyze the (t,p) reactions on ^{20}Ne [6] and ^{18}O [15] at E_t = 15 MeV. The parameters are listed in Table III.

The code CHUCK can handle deformed potentials in inelastic channels as well as spherical potentials as used in DWUCK. Because both ^{20}Ne and ^{22}Ne are deformed nuclei, the (t,p) cross sections could be affected by inelastic scattering via strong channel coupling. Figure 9 displays the calculated angular distributions of the ground state (g.s.), 0^+ and the 4.460-MeV, 2^+ level, using DWUCK and CHUCK. In the CHUCK calculations, we considered the effects of triton inelastic channel coupling and proton inelastic channel coupling between the 0^+ ground state and the first 2^+ level in both ^{20}Ne and ^{22}Ne. The deformation parameters used in these channels were both β_2 = 0.35, which was also used in all other virtual $E2$ transitions. The virtual $E2$ transition potential parameters are listed in Table III, for triton and proton channels separately. Inelastic scattering channels have effects on the (t,p) cross sections of both levels, but the gross features of the cross sections are unchanged (We give more examples in the next section).

The levels in ^{22}Ne could be populated via two-step processes. Three two-step processes might have important contributions to the (t,p) reaction. The first process involves triton inelastic scattering on ^{20}Ne, i.e., an excited state in ^{20}Ne is populated first, then two neutrons are captured to form a level in ^{22}Ne (called triton-inelastic-process, or TIP hereinafter). In the present work, we consider only the first 2^+ level (E_x = 1.63 MeV) in ^{20}Ne because the inelastic scattering cross section of this level is the largest in ^{20}Ne. The second process involves also inelastic scattering, but in the proton channel. In this process, the (t,p) reaction first populates an intermediate level in ^{22}Ne, then a final level is reached via inelastic scattering of the proton (called proton-inelastic-process or PIP hereinafter). We considered a 2^+ intermediate level for 0^+ and 1^+ final levels, a 0^+ or 2^+ intermediate level for 2^+ final levels, a 2^+ or 4^+ intermediate level for 3^+ and 4^+ final levels, a 4^+ intermediate level for 5^+ final levels, and a 1^- or 3^- intermediate level for 1^-, 2^-, and 3^- final levels, in our analysis. Only $E2$ transitions were

considered for inelastic scattering in the proton channel. The last two-step process is a "t-d-p" process, i.e., ^{20}Ne captures a neutron to form an intermediate ^{21}Ne level, then ^{21}Ne captures the second neutron to form a ^{22}Ne level (called t-d-p process, or TDP hereinafter). Two low-lying levels, located at excitation energies 0.351 MeV and 2.794 MeV, with spin-parities of $5/2^+$ and $1/2^+$, respectively, in ^{21}Ne could play important roles in this process because they have larger (d,p) spectroscopic factors than other levels [16]. The optical parameters of the deutron channel were adopted from Ref. [2], where they were used in the analysis of ^{12}C$(t,p)^{14}$C reaction at $E_t = 15$ MeV.

The properties of the low-lying 2s1d shell (positive-parity) levels in ^{22}Ne are predicted remarkably well using the USD interaction [7]. Transfer amplitudes for the (t,p) reaction were calculated using the code OXBASH [17]. Thus comparison between the experimental data and the DWBA results, which were obtained by using the shell-model transfer amplitudes in DWUCK or CHUCK, could then give information on the reaction mechanism. Figure 10 compares theoretical calculations with experimental data for the two of the strongest levels below 9 MeV, viz. the g.s., 0^+ and the 5.367-MeV, 2^+ level. A one-step process (OSP hereinafter) reproduces the data very well (solid lines). The contributions from two-step processes were found to be small for populating these two strong levels.

Cross sections for OSP were calculated to be small in populating some levels, e.g., the first 2^+ (1.279 MeV) and the first 4^+ (3.359 MeV) levels. Experimental angular distributions and theoretical results for these two levels are displayed in Fig. 11. The 2^+ level could be mainly populated via TDP (dashed line), with minor contributions from TIP (dot-dashed line) and PIP (dotted line). The OSP (double-dot-dashed line) is found to be negligible. The TDP (dashed line), as well as OSP (dot-dashed line) have contributions to the 4^+ level. The TIP (dotted line) is weak, and PIP (double-dot-dashed line) is negligible.

Unnatural-parity levels, e.g., the first 2^- (5.148 MeV) and the first 3^+ (5.641 MeV) levels, could be populated only through one of the two-step processes. Shell-model transfer amplitudes are available for the 3^+ level, but not for the negative-parity 2^- level, with the consideration of 2s1d shell space in the present work. We compared only the shapes of the angular distributions of different processes in the analysis for the 2^- level. The theoretical results are compared to the experimental data in Fig. 12. The TDP dominates in populating the 3^+ level, and it is the only mechanism reproducing the angular distribution of the 2^- level.

TABLE I. ^{20}Ne(t,p) results in comparison with previous information below 8 MeV. (E_x in keV, and σ in mb/sr).

Compilation[a]		(t,p)[b]		Present		
E_x	J^π	E_x	L	E_x	σ_{max}	L
0	0^+	0	0	−4(5)	1.6	0
1275	2^+	1275(5)	2	1279(5)	0.22	2
3357	4^+	3359(5)		3359(5)	0.13	4
4457(2)	2^+	4453(5)		4460(5)	0.16	2
5148(2)	2^-			5148(5)	0.07	(1,3)
5326(1)	1^+					
5365(2)	2^+	5360(10)	2	5367(5)	1.4	2
5523(1)	4^+	5522(10)	4	5524(5)	0.22	4
5641(1)	3^+	5643(10)	(1,2)	5641(5)	0.07	(2,4)
5910(2)	3^-	5911(10)		5911(5)	0.13	3
6115(6)	2^+	6115(10)	2	6115(5)	1.2	2
6237(5)	0^+	6238(10)	0	6236(5)	1.6	0
6311(2)	6^+					
6345(1)	4^+	6345(10)		6330(10)[c]	0.28	4
6636(2)	$(2,3)^+$	6642(10)		6636(5)	0.17	2
6691(4)	1^-	6691(10)		6682(10)	0.10	1
6817(2)	2^+	6825(10)		6820(10)	0.10	2
6853(2)	1^+			6856(10)	0.05	(0,2)
6904(9)	$(0,1)^+$	6908(10)		6903(10)	0.09	0
7052(7)	1^-			7050(10)	0.20	1
7341(1)	$(3,4)^+$					
7342(6)	0^+	7345(10)	(4)	7343(10)[d]	1.2	0
7406(2)	$(1,3)^-$	7405(10)		[7414(15)][e]	≤ 0.21	
7423(1)	$(3,5)^+$			[7414(15)][e]	≤ 0.21	
[7470(20)]				[7486(10)][f]	≤ 0.25	(5^-)
7489(6)	1^-	7491(10)	1	[7486(10)][f]	0.25	1
7644(4)	2^+	7643(10)		7639(10)	0.30	2
7664(8)	2^-					
7721(3)	3^-	7726(10)	3	7720(10)	1.5	2
7924(6)	2^+	7924(10)		7925(10)	0.11	2

[a]From Refs. [8] and [9].
[b]From Ref. [6].
[c]The 6311-keV, 6^+ level might be weakly populated.
[d]The 7341-keV, $(3,4)^+$ level might be weakly populated.
[e,f]Not separable levels.

IV. REACTION MECHANISM

For more detailed study of the reaction mechanisms, we considered all four different processes in the analysis of the data for the levels with known spin parities. The best-fit curves (solid lines) are shown in Figs. 2–8. These curves were obtained from one process if a dominant process existed. The cross sections calculated from the coherent sum of the amplitudes from different processes have been used for the clear 2s1d shell levels if no one process was dominant. We assumed one process is dominant for the levels having no shell-model transfer amplitudes. Shown in the figures are also the DWUCK results (dashed lines) for levels with excitation energies lower than 7.5 MeV. We thus could evaluate how good is the one-step DWBA process with spherical potentials in fitting the data. For levels with excitation energies higher than 7.5 MeV, we compared DWUCK calculations only if they fit the data, and indicate those, for which two-step CHUCK calculations were performed, in the text.

A. The 2s1d shell levels

Fourteen low-lying levels ($E_x < 7.7$ MeV) are 2s1d shell levels. The excitation energies, spin parities of these levels are g.s., 0^+_1; 1.279, 2^+_1; 3.359, 4^+_1; 4.460, 2^+_2; 5.367, 2^+_3; 5.524, 4^+_2; 5.641, 3^+_1; 6.115, 2^+_4; 6.236, 0^+_2; 6.330, 4^+_3;

TABLE II. ^{20}Ne(t,p) results in comparison with previous information above 8 MeV. (E_x in keV, and σ in mb/sr).

Compilation[a]		(t,p)[b]		Present		
E_x	J^π	E_x	L	E_x	σ_{max}	L
8081(4)	$(2\text{–}4)^+$	8085(10)		8081(10)	0.05	(4)
8131(7)	2^+	8125(10)		8129(10)	0.09	2
8162(4)	3	8163(10)		8164(10)	0.13	(2,3,4)
8382(7)	$(3^-,4^+)$	8386(10)		8387(10)	0.12	3
8491(2)	2^+	8504(15)		8500(10)	0.11	2
8561(2)	$(1,2)^+$			8545(15)	0.11	2
8592(4)		8593(10)		8590(10)	0.60	(2)
8737(7)	3^-	8738(10)		8743(10)	0.50	3
8861(4)	$(0\text{–}4)^+$	8867(10)		8865(10)	0.10	
8979(9)		8981(10)		8980(10)	0.21	(2,4)
9040(9)				9050(10)	0.14	(4,5)
9097(3)	$(1\text{–}3)^-$	9092(10)		9096(10)	0.53	(1)
9170(4)	$(2\text{–}6)^+$	9179(10)		9181(10)	0.34	4
9223(9)		9225(10)	(3)	9229(10)	1.2	2
9325(9)		9329(10)		9337(10)	0.30	
9505(10)		9505(10)		9510(10)	0.81	(3)
9540(15)		9540(15)		9541(10)	1.5	2
9648(15)	5	9648(15)		9654(10)	0.24	(4,6)
9717(20)				9734(10)	0.14	
9858(20)				9841(10)	0.17	
				10072(10)	0.16	
10132(15)		10132(15)		10142(10)	2.0	2
				10230(15)	0.11	
10299(4)	$\pi = N, \leq 4$	10302(15)		10316(15)	0.32	(2,3)
				10384(15)	0.18	
10474(15)		10474(15)		10466(10)	0.64	3
10493(2)				10504(10)	1.0	2
				10551(15)	0.69	2
10618(3)	$\pi = N$			[10635(15)][c]	(0.15)	(4)
10654(20)	5			[10635(15)][c]	(0.15)	5
10706(6)	$\pi = N$	10711(15)		10720(10)	0.31	
				10820(15)	0.19	
10858(3)	$\pi = N, \leq 4$			10870(10)	0.26	3
10922(3)	1^-			10933(10)	0.86	1
		11063(15)		11064(10)	1.5	2
11161(15)		11161(15)		11173(10)	0.53	3
11271(4)	$(2^+,3^-,4^+)$	11276(15)		11291(15)	0.52	3
11433(6)	$\pi = N$			[11451(15)][d]	≤ 0.58	(3)
11466(3)	1^-			[11451(15)][d]	≤ 0.58	1
11520(15)	7^-	11520(15)		11533(10)	0.50	(7)
11578(5)				11594(15)	0.14	
				11656(10)	0.18	(≥ 6)
11686(5)	2^+			11708(15)	0.16	2^+
		11760(15)		11772(10)	1.3	3
11886(10)	1^-	11895(15)		11907(10)	1.3	≤ 2
12056(10)				12071(15)	0.29	
				12218(15)	0.13	
12380(10)	2^+	12384(15)		12390(10)	1.2	3
				12450(20)	0.27	$(0^+,1^-)$
12610(10)	$(1^-,2^+)$			12643(15)	0.58	≤ 2
				12862(15)	0.17	(3)
				12910(15)	0.26	(2,3)
				13078(20)	0.50	
				13274(20)	0.26	
				13384(15)	0.19	

[a]From Refs. [8] and [9].
[b]From Ref. [6].
[c,d]Not separable levels.

6.636, 2_5^+; 6.856, 1_2^+; 7.343, 0_3^+, and 7.639 MeV, 2_6^+. The subscript i of the spin-parity indicates the ith 2s1d shell level with this spin-parity. All the transfer amplitudes of the (t,p) reactions (including these of OSP, TIP, PIP, and TDP) were calculated using the code OXBASH [17] with the USD interaction [7]. A reasonable reaction mechanism should not only reproduce the experimental angular distribution, but also have a normalization factor close to unity. Here, we define the overall normalization factor $\in$ as

$$\in = \frac{\sigma_{\rm exp}}{\sigma_{\rm th}} = \frac{\sigma_{\rm exp}}{N\sigma_{\rm DWBA}}, \qquad (2)$$

where $\sigma_{\rm DWBA}$ is the DWBA cross section, which was obtained from DWUCK or CHUCK, and $N = 248$ for DWUCK and 2.43×10^6 for CHUCK. The dominant process(es) and normalization factor for each of these levels are listed in Table IV. Also listed in the table are the theoretical excitation energies.

The one-step process was found to be dominant in populating six levels: 0_1^+ (g.s.), 2_2^+ (4.460 MeV), 2_3^+ (5.367 MeV), 2_4^+ (6.115 MeV), 0_2^+ (6.236 MeV), and 0_3^+ (7.343 MeV). Cross sections arising from two-step processes were at most 20% of those from the one-step process for all of these levels. The peak cross sections of five of these levels are larger than 0.5 mb/sr. The only exception is the 2_2^+ level, which has $(d\sigma/d\Omega)_{\rm max}$ about 0.2 mb/sr. However, its angular distribution has a clear one-step character.

The CHUCK calculations are expected to fit the experimental angular distributions better because of the large deformation of ^{20}Ne and ^{22}Ne. Nevertheless, DWUCK also reproduces the experimental angular distributions of these strong levels quite well (dashed lines).

The one-step cross sections were calculated to be small for populating the other eight 2s1d-shell levels. In these cases, two-step processes appeared to compete with the one-step process, or to dominate the reaction. The 3_1^+ level is dominated by TDP, while OSP combining with PIP dominates the 4_2^+ levels. The TIP and PIP make main contributions to the 1_2^+ level. Several processes contribute to the 2_1^+ and 4_1^+ levels, as discussed in the last section.

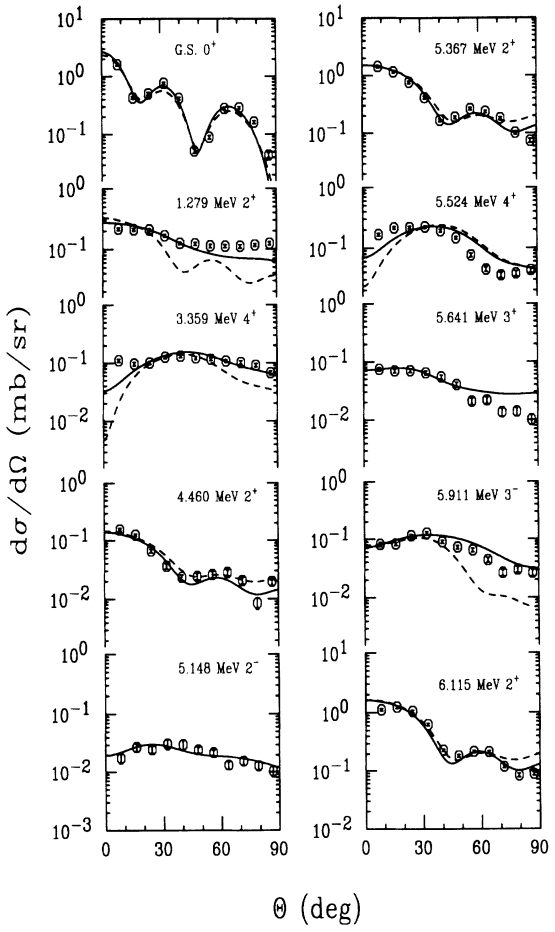

FIG. 2. Angular distributions for the levels between the ground state and the excitation energy of 6.20 MeV. The solid curves are the best fitting curves, the dashed curves are the results of DWUCK calculations, and other curves are the results of CHUCK calculations.

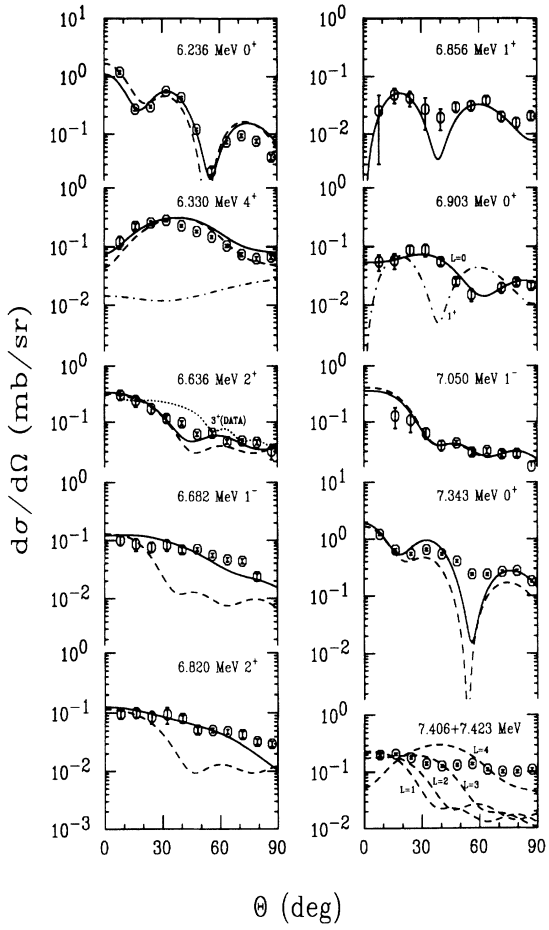

FIG. 3. Same as Fig. 2, but for the levels between 6.20 and 7.45 MeV. The dotted line for the 6.636-MeV level represents the data of the 3^+ level at excitation energy of 5.641 MeV with a normalization factor of 4.

The 4_3^+ (6.330 MeV) level was not separable from the nearby 6^+ (6.311 MeV) level. Our calculation showed that the cross section of the 6^+ level (dashed line, Fig. 3) is much smaller than that of the 4_3^+ level. The theoretical cross section with 4_3^+ alone fitted the data very well. Therefore, the measured peak at $E_x = 6.330$ MeV is primarily due to the previously-known 4_3^+ (6.345 MeV) level. A one-step process (DWUCK, dashed line) provides a good fit to the angular distribution shape. However, OSP plus TIP fitted the data very well and with a better normalization factor (1.5 vs 2.9). Therefore, this level was likely populated through the above two processes.

The 6.636-MeV level was assigned as $(2^+, 3^+)$ previously [8]. The CHUCK result using the 2_5^+ transfer amplitudes fitted the data very well, whereas curve (dotted) drawn through data for the lower 3_1^+ level, with a normalization factor of 4, did not. A reasonable normalization factor was also obtained ($\epsilon = 0.3$). The OSP and TIP dominate in populating this level. Calculations for the theoretical 3_2^+ level did not fit the cross section at forward angles, and had too large a normalization factor ($\epsilon = 18$) although the normalization factor was not a good indicator for TDP. Therefore, this level is probably the 2_5^+ 2s1d shell level, which corresponds to a theoretical excitation energy of 6.570 MeV.

The measured peak at $E_x = 7.639$ MeV (Fig. 4) might have contributions from the 7.644-MeV, 2^+, and 7.664-MeV, 2^- levels. The uncertainty in excitation energies at this energy region is about 5 keV. The excitation energy of 7.639 MeV is far from the 7.664 ± 0.008 MeV level. Furthermore, the differential cross section of the 7.664-MeV level would probably be smaller than 0.1 mb/sr because it is an unnatural-parity level. We assumed that the measured cross section was mainly from the 7.644-MeV, 2^+ level. Our calculation showed that this could be the sixth 2^+ 2s1d-shell level corresponding to a theoretical excitation energy of 7.799 MeV. The TIP result using shell-model amplitudes fitted the data, and gave a normalization factor of 1.5.

B. Other levels

Seventeen levels, with known J^π's but no available shell-model counterparts were observed (see Table V).

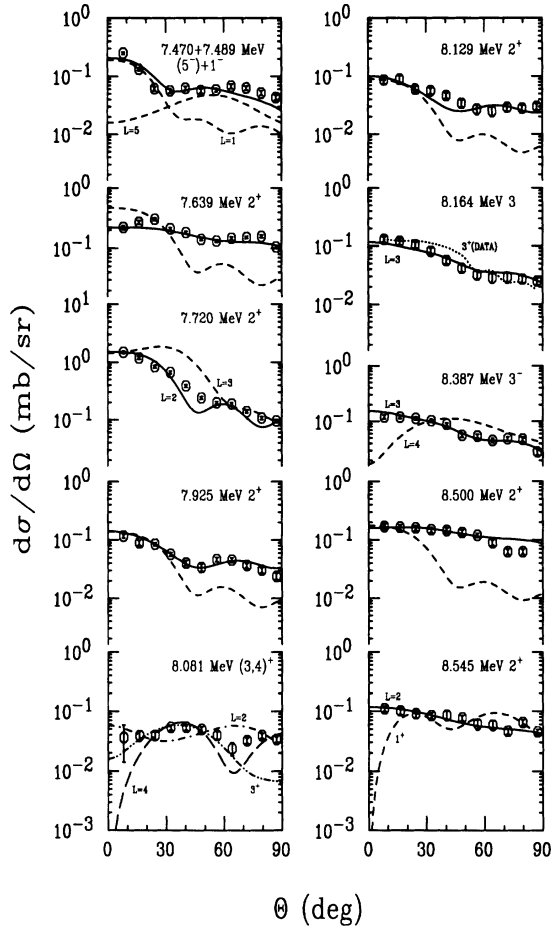

FIG. 4. Same as Fig. 2, but for the levels between 7.45 and 8.55 MeV. For OSP mechanism, only DWUCK was used in the calculations for the levels above 7.45 MeV. The dotted line at 8.164 MeV represents the data of the 3^+ level at excitation energy of 5.641 MeV with a normalization factor of 1.5.

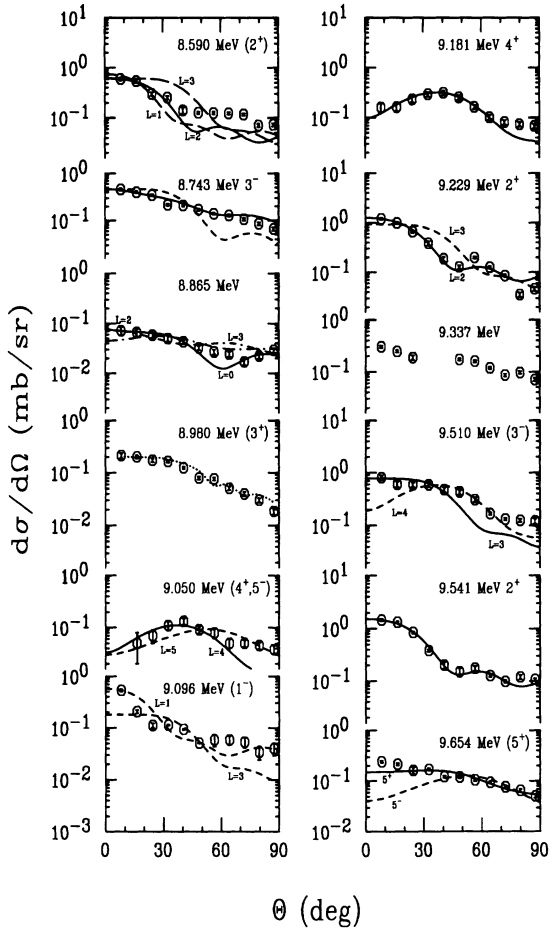

FIG. 5. Same as Fig. 4, but for the levels between 8.55 and 9.70 MeV. The dotted line at 8.980 MeV represents the data of the 3^+ level at excitation energy of 5.641 MeV with a normalization factor of 2.8.

The excitation energies and spin-parities of these levels are 5.148, 2^-; 5.911, 3^-; 6.682, 1^-; 6.820, 2^+; 7.050, 1^-; 7.486, 1^-; 7.720, 3^-; 7.925, 2^+; 8.129, 2^+; 8.500, 2^+; 8.743, 3^-; 10.933, 1^-; 11.466, 1^-; 11.533, 7^-; 11.708, 2^+; 11.907, 1^-; and 12.390 MeV, 2^+. In the present work, angular distributions for these levels were calculated by using pure configurations. Unless indicated in the following paragraphs, we used a $(d_{5/2})^2$ or $(f_{7/2})^2$ configuration in the calculations of the cross sections for the 2^+ and 4^+ levels; $(d_{5/2}p_{3/2})$ for the 1^- and 3^- levels; and $(f_{7/2}g_{9/2})$ for the 7^- level. These simplifications did not affect the results because different configurations in the same major shell (i.e., 2s1d or 1f2p shell) gave different absolute values of the cross sections, but similar angular distributions. One-step process, and TIP, PIP, and TDP were considered in this order of priority.

Among the 17 levels, seven strongly populated levels (E_x = 7.050, 7.486, 7.720, 10.933, 11.466, 11.907, and 12.390 MeV) appear to be dominated by the one-step process. Five of these seven levels were assigned to have the same spin-parities as in Refs. [8] and [9]. The measured 7.486-MeV peak is a combination of the previous 7.470- and 7.489-MeV levels, the latter of which is a 1^- level. The angular distribution of this peak showed strong evidence of the 7.489-MeV, 1^- level at forward angles. At larger angles, the contribution from the 7.470-MeV level dominated, indicating that the 7.470-MeV level probably has $J > 4$. Figure 4 shows angular distribution for 1^- and 5^- levels and their sum. The 11.466-MeV, 1^- level was unresolved from the 11.433-MeV, natural-parity level. The observed peak at E_x = 11.451 MeV is 18 keV away from the previous 11.433-MeV level and 15 keV from the 11.466-MeV level. This indicates that the measured peak at excitation energy of 11.451 MeV is a mixture of the above two levels. We fitted the experimental angular distribution excellently by combining 1^- and 3^- theoretical angular distributions (Fig. 7). Even though the angular distribution for the level at 11.907 MeV (Fig. 8) agrees with 1^-, we assigned its spin-parity to be $(1^-, 2^+)$ in the present work, because we could not eliminate a 2^+ possibility from its angular distribution alone.

The angular distributions of the other two strong levels could not be fitted by using the assigned spin-parities in Ref. [8]. The 7.720-MeV level had a spin-parity assignment of 3^-. Our (t,p) cross section for this level has a very similar angular distribution as that of a 2^+ level (solid line, Fig. 4). This result is contrary to the

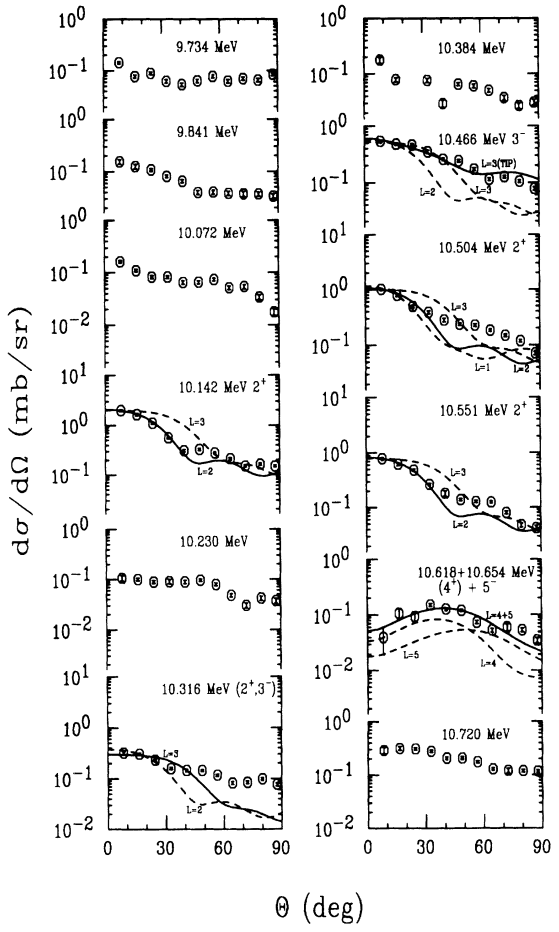

FIG. 6. Same as Fig. 4, but for the levels between 9.70 and 10.80 MeV.

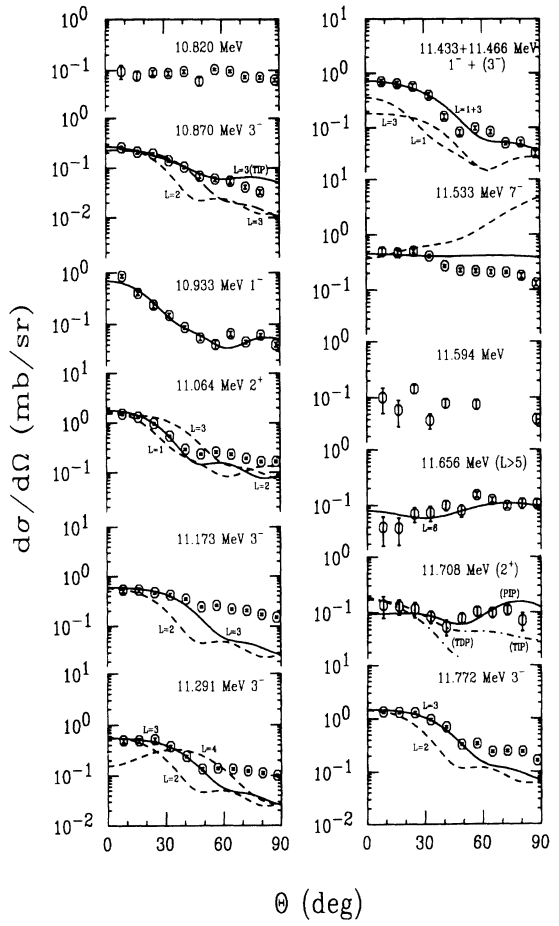

FIG. 7. Same as Fig. 4, but for the levels between 10.80 and 11.80 MeV.

(d,p) [16], (^{6}Li,d) and (^{7}Li,t) [8] results, but not to $(\alpha,p\gamma)$ and gamma decay [9]. On the other hand, the spin-parity of the 12.390-MeV level was assigned to be 2^+ from the $^{18}O + \alpha$ reaction [9], but its angular distribution here shows strong 3^- character (Fig. 8). We prefer to assign it as a 3^- level in the present work according to its angular distribution.

The other ten levels are likely populated through one of the two-step processes. Seven levels (E_x = 5.911, 6.682, 6.820, 7.925, 8.129, 8.500, and 8.743 MeV) were populated through TIP, two levels (E_x = 5.148 and 11.533 MeV) through TDP, and one level (E_x = 11.708 MeV) via PIP. We obtained good fits for nine of the levels but not for the 7^- level at 11.533 MeV (Fig. 7). This 7^- level could not be fitted well with any combination of the four processes. It might be populated via another reaction mechanism, for example, compound reaction, because of its large J.

Below an excitation energy of 8 MeV, the 2^+ levels could be sd-shell levels. However, the 6.820- and 7.925-MeV levels were fitted badly using the transfer amplitudes for 2^+_5 and 2^+_6, respectively (not shown in the figures). We obtained a normalization factor of 0.12 for the 6.820-MeV level, and a poor angular distribution for the 7.925-MeV level. Therefore, we calculated the cross sections of them using pure configurations. The 6.820-MeV level could be fitted using an $(f_{7/2})^2$ configuration. This perhaps indicates that it might be the first 1f2p-shell 2^+ level. The 7.925-MeV level was fitted using a $(d_{5/2})^2$ configuration. Accordingly, we chose the 6.636- and 7.644-MeV levels as the 2s1d-shell 2^+_5 and 2^+_6 levels, respectively, in the discussion of 2s1d-shell levels.

From the analysis of all 31 levels with known spin parity, we found that angular distributions with $(d\sigma/d\Omega)_{\max} > 0.5$ mb/sr were fitted using a one-step process. For the more weakly populated levels [$(d\sigma/d\Omega)_{\max} \leq 0.5$ mb/sr], two-step processes may play important roles. In the case of $(d\sigma/d\Omega)_{\max} \leq 0.1$ mb/sr, two-step processes were found to be the dominant reaction mechanisms.

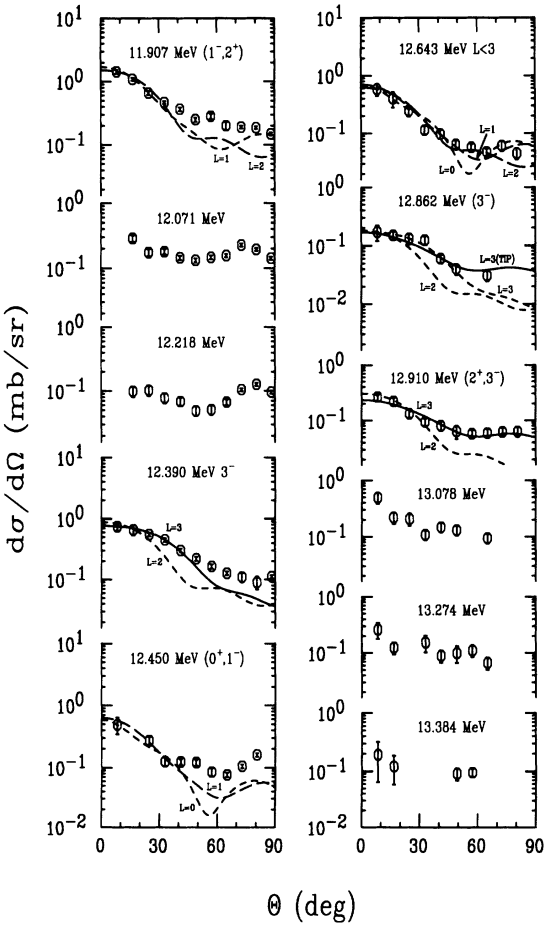

FIG. 8. Same as Fig. 4, but for the levels between 11.80 and 13.4 MeV.

V. SPIN-PARITY ASSIGNMENTS

Having the above knowledge, we could assign spin-parities to some of the other levels we observed in this measurement (see Table V). However, uncertainty still exists because of many possible two-step processes. One angular distribution could be fitted using different final spin parities by choosing different two-step processes. To reduce the uncertainty, we assigned spin parities to the levels with tentative spin parities [8] or those strongly populated [$(d\sigma/d\Omega)_{\max} > 0.5$ mb/sr] in the reaction. For levels with tentative spin parities, we considered all the possible final spin parities and four different reaction mechanisms in the calculations. For the strongly populated levels with no previous spin-parity assignment, we took a one-step process as the main reaction mechanism. The resulting spin parities should be reliable because the angular distributions of the one-step (t,p) cross sections have distinctive characters. Again, we used $(d_{5/2})^2$ or $(f_{7/2})^2$ configuration in the calculations for the cross sections of 0^+, 2^+, and 4^+ levels; $(f_{7/2})^2$ for 6^+ levels; $(d_{5/2}p_{3/2})$ for 1^- and 3^- levels; and $(d_{5/2}f_{7/2})$ for 5^- levels.

A. Levels with tentative spin parities

Besides the 6.636-MeV, 2^+_5 level (discussed in the last section), we observed 19 levels which had been assigned tentative spin parities from previous measurements [8]. Shown in Figs. 3 to 8 are the fits for these levels. In the following paragraphs, we discuss these levels in detail separately.

6.903 MeV (Fig. 3). The angular distribution of this level has no 1^+ feature. It is fitted very well using one-step process with $(f_{7/2})^2_{L=0}$ configuration (solid line). This indicates the level is probably the first 0^+ level in the 1f2p shell.

7.406 and 7.423 MeV (Fig. 3). These two levels cannot be separated in the measurement. The excitation energy of the peak corresponding to the pair was determined as

TABLE III. Potential parameters used in the DWBA calculations. Strengths are in MeV, lenths in fm.

Channel	V	W	$W' = 4W_D$	V_{so}	$r_0 = r_{so}$	$a = a_{so}$	r'_0	a'	r_{0c}
t[a]	162.9	17.9	0	0	1.16	0.69	1.50	0.82	1.18
d[b]	94.3	0	35.0	7.0	1.172	0.807	1.357	0.807	1.18
p[a]	54.0	0	60.0	0	1.25	0.65	1.25	0.47	1.25
n[a]	varied	0	0	$\lambda = 25$	1.25	0.65	...	...	...
t'[c]	55.0				1.27	0.35			
p'[c]	55.0				1.27	0.35			

[a]From Refs. [12] and [13], parameters were also used for the inelastical channels.
[b]The deutron parameters used in CHUCK to calculate the TDP two-step reaction mechanism [2].
[c]For virtual $E2$ transitions only, $\beta_2 = 0.35$.

7.414 MeV. Because of the small absolute cross section and featureless angular distribution, we could not assign spin parities to these two levels (the theoretical results for $L = 1 - 4$ are displayed in Fig. 3).

8.081 MeV (Fig. 4). No 2^+ angular distribution could fit the data. An example of it with TIP is shown, along with a 4^+ angular distribution using OSP and a 3^+ angular distribution with TIP. The 4^+ and 3^+ angular distributions fit the data fairly. Therefore, this level could be a $(3^+, 4^+)$ level.

8.164 MeV (Fig. 4). The 3^- TIP angular distribution fits the data very well. On the other hand, it has about the same angular distribution as that of the 5.641-MeV, 3^+ level (dotted line). And the absolute cross section of the 8.164-MeV level is only 50% larger than that of the 5.641-MeV level. Therefore, we could not make a parity

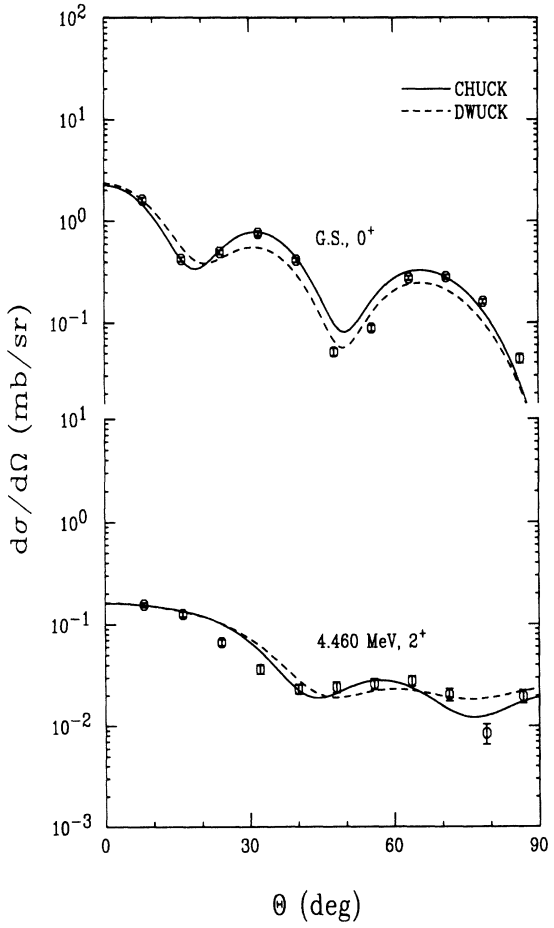

FIG. 9. Comparison of the one-step DWBA results from CHUCK and DWUCK for the ground state, 0^+ and the 4.460-MeV, 2^+ level.

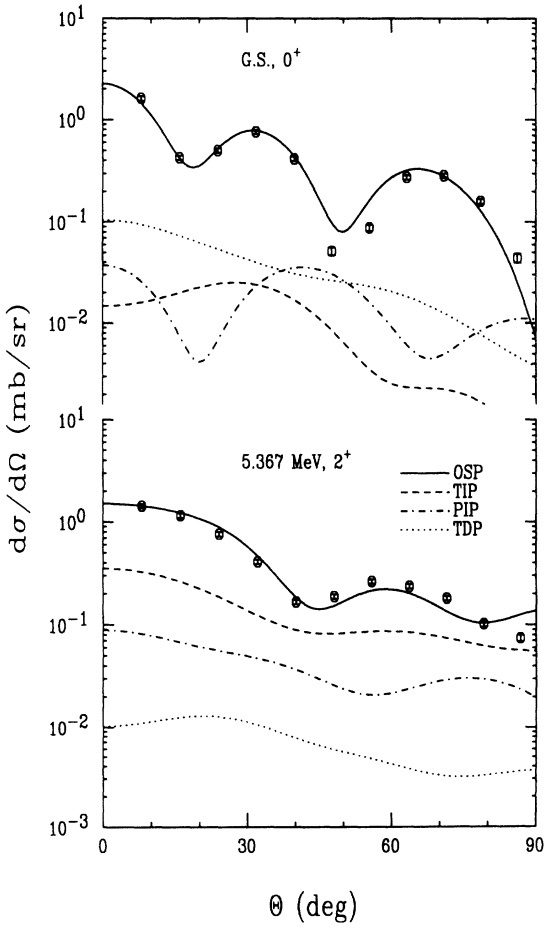

FIG. 10. The g.s., 0^+; and 5.367-MeV, 2^+ level were populated through the OSP. Their angular distributions were fitted by using the OSP. Two-step process contributions are ignorable.

assignment to this level.

8.387 MeV (Fig. 4). A spin parity of 3^- is preferred for this level because its angular distribution is not characteristic of 4^+.

8.545 MeV (Fig. 4). No 1^+ angular distribution could fit the data, but a TIP 2^+ angular distribution reproduces the measured one. This level, therefore, is probably a 2^+ level.

8.865 MeV (Fig. 5). Even though some theoretical calculations with $L \leq 4$ could reproduce the experimental angular distribution, we make no spin-parity assignment because of its featureless character.

9.096 MeV (Fig. 5). This is a 1^- level from the angular distribution and the magnitude of the cross section ($\sigma_{max} = 0.53$ mb/sr). The maxium cross section of a 2^- level should be much smaller than 0.5 mb/sr, and a 3^- angular distribution is very different from the measured one.

9.181 MeV (Fig. 5). The observed 9.181-MeV peak, corresponding to the previous 9.170(4)-MeV level [8], clearly has $J^\pi = 4^+$. The nearby 9.178-MeV, 1^+ level does not contribute significantly to the cross section.

9.654 MeV (Fig. 5). The forward angle cross sections of this level favor a spin parity of 5^+ rather than 5^-. Therefore it is probably a (5^+) level from the angular distribution alone.

10.316 MeV (Fig. 6). From the angular distribution, it is more likely a 3^- level, but 2^+ is also a possible spin parity for it. We assigned the tentative spin-parity of this level to be $(2^+, 3^-)$.

10.618 and 10.654 MeV (Fig. 6). These two levels were not separable in the measurement. The 10.618-MeV level had been assigned to have natural parity, and the 10.654-MeV level has $J = 5$ from previous measurments. The measured excitation energy is 10.635 MeV in the present work. Its experimental angular distribution shows both are likely natural parity levels with high spins. We combined 4^+ and 5^- theoretical distribution (the magnitude of the 4^+ level is a factor of 2 larger than that of the 5^- level), and fitted the data very well. Thus, we assign 5^-

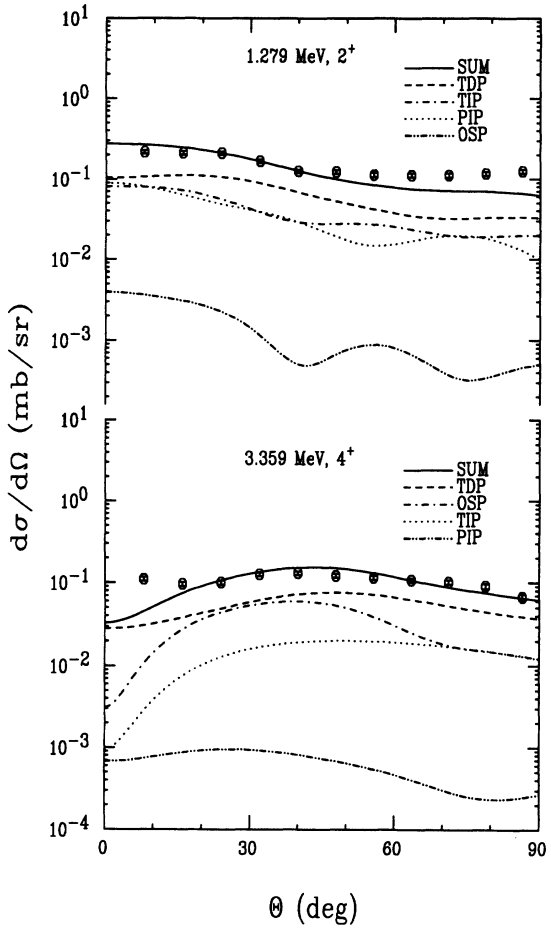

FIG. 11. The 1.279-MeV, 2^+; and 3.359-MeV, 4^+ levels were populated via more than one process. Two-step processes may dominate, while OSP could be small enough to be ignored.

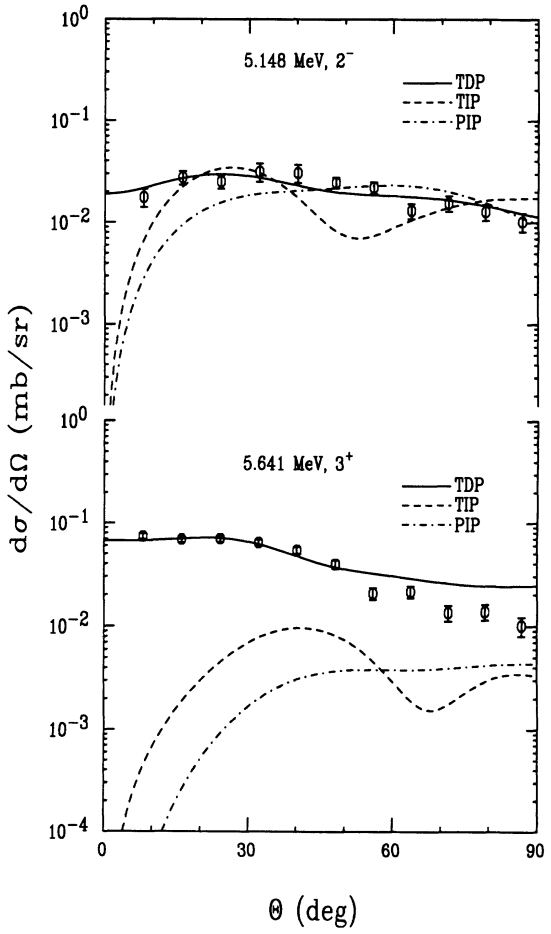

FIG. 12. The angular distributions of two unnatural parity levels (5.148 MeV, 2^-; and 5.641 MeV, 3^+). The TDP dominated in populating these two levels. OSP is forbidden because of violation of selection rules.

TABLE IV. Normalization factors and reaction mechanisms for the 2s1d-shell levels.

J^π	E_x (keV) Compilation[a]	E_x (keV) Present	E_x (keV) Theory[b]	$\epsilon = \frac{\sigma_{exp}}{\sigma_{th}}$ DWUCK	$\epsilon = \frac{\sigma_{exp}}{\sigma_{th}}$ CHUCK
0^+_1	0	−4	0	1.5	1.8(OSP)
2^+_1	1275	1279	1367	32	0.6(TDP+TIP+PIP)
4^+_1	3357	3359	3377	1.4	0.6(TDP+OSP+TIP)
2^+_2	4457	4460	4450	4.0	7.0(OSP)
2^+_3	5365	5367	5027	0.6	1.1(OSP)
4^+_2	5523	5524	5474	1.2	1.0(OSP+PIP)
3^+_1	5641	5641	5632		1.9(TDP)
2^+_4	6115	6115	6175	0.3	0.5(OSP)
0^+_2	6237	6236	6337	3.9	3.1(OSP)
4^+_3	6345	6330[c]	6424	2.8	1.5(OSP+TIP)
2^+_5[d]	6636	6636	6570	0.2	0.3(OSP+TIP)
1^+_2	6853	6856	6660		2.5(TIP+PIP)
0^+_3	7342	7343	7260	1.6	1.8(OSP)
2^+_6	7644	7639	7799	8.5	1.5(TIP)

[a]From Ref. [8].
[b]Calculated from OXBASH [17] using the USD interaction [7].
[c]The 6311-keV, 6^+ level might be weakly populated.
[d]Spin was assigned as $(2,3)^+$ in Ref. [8].

TABLE V. Reaction mechanisms and spin-parity assignments in comparison with compilation.

Compilation[a] E_x (keV)	Compilation[a] J^π	Present E_x (keV)	Present J^π	DWUCK Configurations	CHUCK Process
5148	2^-	5148	2^-		TDP
5910	3^-	5911	3^-	$d_{5/2}p_{3/2}$	TIP
6691	1^-	6682	1^-	$d_{5/2}p_{3/2}$	TIP
6817	2^+	6820	2^+	$(f_{7/2})^2$	TIP
6904	$(0,1)^+$	6903	0^+	$(f_{7/2})^2$	
7052	1^-	7050	1^-	$d_{5/2}p_{3/2}$	OSP
7406	$(1,3)^-$	(7414)[b]			
7423	$(3,5)^+$	(7414)[b]			
7470		(7486)[c]	(5^-)	$d_{5/2}f_{7/2}$	
7489	1^-	(7486)[c]	1^-	$d_{5/2}p_{3/2}$	
7721	3^-	7720	2^+	$(d_{5/2})^2$	
7924	2^+	7925	2^+	$(d_{5/2})^2$	TIP
8081	$(2\text{–}4)^+$	8081	$(3,4)^+$	$(d_{5/2})^2_{4^+}$	TIP_{3+}
8131	2^+	8129	2^+	$(d_{5/2})^2$	TIP
8162	3	8164	3	$data_{3+}$	TIP_{3-}
8382	$(3^-,4^+)$	8387	3^-		TIP
8491	2^+	8500	2^+	$(d_{5/2})^2$	TIP
8561	$(1,2)^+$	8545	2^+		TIP
8592		8590	(2^+)	$(d_{5/2})^2$	
8737	3^-	8743	3^-	$d_{5/2}p_{3/2}$	TIP
8861	$(0\text{–}4)^+$	8865			
8979		8980	(3^+)	data	
9040		9050	$(4^+,5^-)$	$(d_{5/2})^2, d_{5/2}f_{7/2}$	
9097	$(1\text{–}3)^-$	9096	(1^-)	$d_{5/2}p_{3/2}$	
9170	$(2\text{–}6)^+$	9181	4^+	$(d_{5/2})^2$	
9223		9229	2^+	$(d_{5/2})^2$	
9325		9337			
9505		9510	(3^-)	$d_{5/2}p_{3/2}$	
9540		9541	2^+	$(d_{5/2})^2$	
9648	5	9654	(5^+)		TDP
9717		9734			
9858		9841			
		10072			
10132		10142	2^+	$(d_{5/2})^2$	
		10230			

TABLE V. (*Continued*).

Compilation[a]		Present		DWUCK	CHUCK
E_x (keV)	J^π	E_x (keV)	J^π	Configurations	Process
10299	$\pi = N, \leq 4$	10316	$(2^+, 3^-)$	$(d_{5/2})^2, d_{5/2}p_{3/2}$	
		10384			
10474		10466	3^-	$d_{5/2}p_{3/2}$	TIP
10493		10504	2^+	$(d_{5/2})^2$	
		10551	2^+	$(d_{5/2})^2$	
10618	$\pi = N$	(10635)[d]	(4^+)	$(d_{5/2})^2$	
10654	5	(10635)[d]	5^-	$d_{5/2}f_{7/2}$	
10706	$\pi = N$	10720			
		10820			
10858	$\pi = N, \leq 4$	10870	3^-	$d_{5/2}p_{3/2}$	TIP
10922	1^-	10933	1^-	$d_{5/2}p_{3/2}$	
11063[f]		11064	2^+	$(d_{5/2})^2$	
11161		11173	3^-	$d_{5/2}p_{3/2}$	
11271	$(2^+, 3^-, 4^+)$	11291	3^-	$d_{5/2}p_{3/2}$	
11433	$\pi = N$	(11451)[e]	(3^-)	$d_{5/2}p_{3/2}$	
11466	1^-	(11451)[e]	1^-	$d_{5/2}p_{3/2}$	
11520	7^-	11533	$[7^-]$[g]	$f_{7/2}g_{9/2}$	TDP
11578		11594			
		11656	(≥ 6)	$(f_{7/2})^2_{L=6}$	
11686	2^+	11708	2^+		PIP
11760[f]		11772	3^-	$d_{5/2}p_{3/2}$	
11886	1^-	11907	$(1^-, 2^+)$	$(d_{5/2})^2, d_{5/2}f_{7/2}$	
12056		12071			
		12218			
12380	2^+	12390	3^-	$d_{5/2}p_{3/2}$	
		12450	$(0^+, 1^-)$	$(d_{5/2})^2, d_{5/2}p_{3/2}$	
12610	$(1^-, 2^+)$	12643	$\pi = N, \leq 2$	$(d_{5/2})^2, d_{5/2}p_{3/2}$	
		12862	(3^-)	$d_{5/2}p_{3/2}$	TIP
		12910	$(2^+, 3^-)$	$(d_{5/2})^2_{L=2}$	$\text{TIP}_L = 3$
		13078			
		13274			
		13384			

[a]From Refs. [8] and [9].
[b–e]Not separable from each other.
[f]From Ref. [6].
[g]No good fit for this level.

to the 10.654-MeV level and tentative spin-parity (4^+) to the 10.618-MeV level.

10.720 MeV (Fig. 6). No spin parity could be assigned to this level again because of the absence of distingishing features in its angular distribution.

10.870 MeV (Fig. 7). This level has a 3^- angular distribution. Both OSP and TIP can fit its angular distribution well. We assigned this level as a 3^- level even though it has rather a small absolute cross section ($\sigma_{\max} = 0.3$ mb).

11.291 MeV (Fig. 7). Again this is a 3^- level because of its absolute cross section and angular distribution shape.

11.433 MeV (Fig. 7). It could not be separated from the 11.466-MeV, 1^- level, and has been mentioned in the last section [and tentatively assigned (3^-)] when we discussed the 11.466-MeV level.

12.643 MeV (Fig. 8). Calculated angular distributions for 0^+, 1^-, and 2^+ fit the data fairly. Thus we can only give a limitation of $L \leq 2$ with natural parity.

B. Levels with unknown spin parities

We observed 31 levels which had no spin-parity assignments. Spin-parities were assigned to 12, which have very distinctive angular distributions. Seven of them have been assigned spin parities of 2^+. They are located at E_x = 8.590, 9.229, 9.541, 10.142, 10.504, 10.551, and 11.064 MeV. Five levels have been assigned spin-parities of 3^-, located at E_x = 9.510, 10.466, 11.173, 11.772, and 12.862 MeV. The maximun cross sections of 11 of the 12 levels are larger than 0.5 mb/sr. For these levels, we considered only a one-step process in the fitting. Because the gross features of the angular distributions from DWUCK and CHUCK using OSP are about the same, shown in Figs. 5 to 8 are the results from DWUCK for the 11 strongly populated levels. The 12.862-MeV level (Fig. 8) has a 3^- angular distribution, but a small absolute cross section [$(d\sigma/d\Omega)_{\max} \simeq 0.3$ mb/sr]. We used both OSP and TIP to fit the data. The agreement of the

angular distributions between DWBA result and the experimental data was remarkable. Therefore, spin parity of 3^- was assigned to this level.

We also constrained the spin parities of six other levels at excitation energies (in MeV) and with tentative spin-parities of 7.470, ($L > 4$); 8.980, (3^+); 9.050, ($4^+, 5^-$); 11.656, (≥ 6); 12.450, ($0^+, 1^-$); and 12.910 ($2^+, 3^-$). Among them the 8.980-MeV level has the same angular distribution as that of the 5.641-MeV, 3^+ level, and only a factor of 1.8 larger absolute cross section. From the shell-model calculation, a 3^+ level should appear at about $E_x = 9$ MeV. The 8.980-MeV level is the best candidate for a 3^+ level in this energy region.

The gross features of the differential cross sections for high-spin levels are different from those of low-spin levels. However, for different high-spin levels, the angular distributions are similar and relatively featureless, and have small cross sections. Therefore, spin-parity assignments are more difficult for high-spin levels than for lower spin levels. We assigned spin ≥ 6 only to the 11.656-MeV level in the present work.

VI. DISCUSSIONS AND CONCLUSIONS

The ^{20}Ne(t,p) reaction was measured at $E_t = 15$ MeV in the angle range from 7.5° to 82.5° in steps of 7.5°. Eighty-one ^{22}Ne levels were identified up to an excitation energy of 13.4 MeV.

Angular distributions for 62 levels were well fitted using DWBA results. Theoretical calculations were performed using both spherical and deformed potentials, but the latter do not affect the gross features of the differential cross sections.

A one-step reaction is found to be the dominant reaction mechanism in populating levels with $(d\sigma/d\Omega)_{\max} \geq 0.5$ mb/sr. However, two-step reaction played important roles in the ^{20}Ne(t,p) reaction for other levels. We found that two-step processes could compete with one-step process (or even dominate the reaction) in populating 24 levels among 46 with known (or tentative) spin-paritiy to which we assigned spin-parities. It was shown that two-step processes may not be ignored when $(d\sigma/d\Omega)_{\max} < 0.5$ mb/sr in the ^{20}Ne(t,p) reaction. When a triton bombards the target ^{20}Ne nucleus, it easily excites the first 2^+ level. Therefore, the triton inelastic scattering two-step process was the main two-step process (21 levels among 27, which were probably populated via two-step processes, have significant contributions from TIP).

If the 7^- (11.533-MeV) level was populated through a compound reaction mechanism, the cross sections of some other levels might contain compound contributions. Assuming a compound reaction dominated in populating the 7^- level, it would contribute to the cross sections of low-spin levels at most about $0.4 \times (2J + 1)/15 = 0.027(2J + 1)$ mb/sr. This means compound reactions might contribute cross sections of 0.19 mb/sr for $J = 3$ levels and 0.14 mb/sr for $J = 2$ levels. These values are much smaller than the experimental cross sections for the levels which were assigned spin parities in the present work. Therefore, a compound reaction did not affect the angular distributions of strongly populated low-spin levels.

This work was supported by the National Science Foundation.

[1] D.J. Crozier and H.T. Fortune, Phys. Rev. C **11**, 308 (1975).
[2] S. Mordechai, H.T. Fortune, G.E. Moore, M.E. Cobern, R.V. Kollarits, and R. Middleton, Nucl. Phys. **A301**, 463 (1978).
[3] H.T. Fortune, G.E. Moore, L. Bland, M.E. Cobern, S. Mordechai, and R. Middleton, Phys. Rev. C **20**, 1228 (1979).
[4] S. Truong and H.T. Fortune, Phys. Rev. C **28**, 977 (1983).
[5] D.J. Crozier, H.T. Fortune, R. Middleton, and J.L. Wiza, Phys. Rev. C **11**, 393 (1975).
[6] E.R. Flynn, O. Hansen, and O. Nathan, Nucl. Phys. **A228**, 189 (1974).
[7] B.H. Wildenthal, private communication.
[8] P.M. Endt, Nucl. Phys. **A521**, 1 (1991).
[9] P.M. Endt and C. Van der Leun, Nucl. Phys. **A310**, 1 (1979).
[10] P.D. Kunz, DWUCK computer code, University of Colorado, 1981, unpublished.
[11] P.D. Kunz, CHUCK computer code, University of Colorado, 1974, unpublished.
[12] J. Garrett and O. Hansen, Nucl. Phys. **A212**, 600 (1973).
[13] J. Garrett, R. Middleton, D.J. Pullen, S.A. Andersen, O. Nathan, and Ole Hansen, Nucl. Phys. **A164**, 449 (1971).
[14] F. Perey, Phys. Rev. **131**, 745 (1965).
[15] S. Lafrance, H.T. Fortune, S. Mordechai, M.E. Cobern, G.E. Moore, R. Middleton, W. Chung, and B.H. Wildenthal, Phys. Rev. C **20**, 1673 (1979).
[16] P. Neogy, R. Middleton, and W. Scholz, Phys. Rev. C **6**, 885 (1972).
[17] B.A. Brown, A. Etchegoyen, and W.D.M. Rae, OXBASH, private communication.